Strain and Structure Driven Complex Magnetic Ordering of a CoO Overlayer on Ir(100)

F. Mittendorfer,[1] M. Weinert,[2,*] R. Podloucky,[3] and J. Redinger[1]

[1]*Institute of Applied Physics, Vienna University of Technology, Gusshausstr. 25/134, 1040 Vienna, Austria*
[2]*Department of Physics, University of Wisconsin-Milwaukee, Milwaukee, Wisconsin 53201, USA*
[3]*Institute of Physical Chemistry, University of Vienna, Sensengasse 8, 1090 Vienna, Austria*

(Received 23 March 2012; published 2 July 2012)

We investigate the magnetic ordering in the ultrathin $c(10 \times 2)$ CoO(111) film supported on Ir(100) on the basis of *ab initio* calculations. We find a close relationship between the local structural properties of the oxide film and the induced magnetic order, leading to alternating ferromagnetically and antiferromagnetically ordered segments. While the local magnetic order is directly related to the geometric position of the Co atoms, the mismatch between the CoO film and the Ir substrate leads to a complex long-range order of the oxide.

DOI: 10.1103/PhysRevLett.109.015501 PACS numbers: 61.46.−w, 75.70.Ak

The adsorption of an ultrathin magnetic oxide film, such as CoO, on a nonmagnetic substrate offers a rich and fascinating playground for studying the interplay of the geometrical structure and the magnetic properties. Especially, if the stable surface orientation of the oxide film differs from the substrate, the structural deformations of the oxide film and the magnetic order are closely related. This relation can be observed in the case of a CoO(111) layer supported on Ir(100), where the pseudohexagonal atomic arrangement of the oxide film has to adapt to the square structure of the Ir(100) substrate surface. Due to the large lattice mismatch of about 9.8% between the bulk lattice parameters of CoO(111) and Ir(100), epitaxial growth of the CoO overlayer is very unfavorable. For the related formation of Co_xO_y [1] and Mn_xO_y [2,3] films on Pd(100) surfaces, this lattice mismatch is compensated by the creation of Co vacancies, reducing the stoichiometry of the CoO film. Nevertheless, for the adsorption of CoO(111) on Ir(100), the CoO film yields the bulk stoichiometry, but is expanded to a $c(10 \times 2)$ overlayer, where 9 formula units of CoO are supported on 10 square unit cells of Ir(100) (Fig. 1). The strain-induced relaxations in the CoO overlayer lead to sizable structural inhomogeneities, i.e., distorted bond angles, different bond lengths, buckling, and different local environments with respect to the substrate geometry. Evidently, these structural properties influence both the local and long-range magnetic ordering of the CoO overlayer, resulting in complex magnetic patterns.

In recent years, density functional theory (DFT) approaches have evolved as powerful tools to complement the experimental efforts to resolve the atomic structure of supported surface oxides [4–6], and to analyze the underlying electronic structure and the concomitant magnetic ordering. In this Letter, we present extensive DFT calculations for two different CoO $c(10 \times 2)$ overlayer structures supported on Ir(100). In addition, we demonstrate that the close relationship between the magnetic configurations and the structural deformations is already present in simplified models of the system, thus, illustrating the driving mechanism for the magnetic ordering.

DFT calculations were performed using the Vienna *ab initio* simulation package (VASP) [7,8] in the projector augmented wave framework [9]. The exchange correlation functional was described by the general gradient approximation of Perdew-Burke-Ernzerhof (PBE) [10]. To account for the localized d states of the cobalt atoms, the PBE + U approach of Dudarev [11] was used. Varying U-J in the range between 0 to 4 eV, we find that a value of U-$J = 1$ eV leads to the best agreement with the calculated geometric structure of the CoO/Ir(100) system with experiment [12]. Changing U-J from 1 to 3 eV leads to an increase of the average Co moment from 2.13 to 2.45 μ_B but does not change the magnetic ground state. However, the larger value of U-J increases the Co-Ir distance by as much as 0.33 Å, in clear contrast to the experimental finding. The same value of U-$J = 1$ eV was found to yield a bulk volume very close to experiment and also describes the electronic structure satisfactorily compared to a more sophisticated, but very costly, approach using hybrid functionals [13]. If not stated otherwise, all results of the present work refer, therefore, to this choice of U-$J = 1$ eV.

A repeated slab model was used consisting of five Ir layers and CoO overlayers on both sides of the Ir slab and a separating vacuum of 17 Å, thus avoiding dipolar interaction between the repeated slabs. A Monkhorst–Pack type k mesh of $11 \times 11 \times 1$ was used for small cells, and a $4 \times 4 \times 1$ k mesh for the $c(10 \times 2)$ structures; doubling the k mesh in the latter case changes the Co moments by less than 0.03 μ_B. In all calculations, the structural degrees of freedom are fully relaxed.

Recently, an atomistic model has been proposed for the $c(10 \times 2)$ CoO(111) layer on Ir(100) surface on the basis of LEED experiments [12]. In this study, 59 structural parameters had to be optimized to obtain a satisfactory fit, demonstrating the complexity of the system, and calling for corroboration by an up-to-date DFT approach such as applied

in this work. Most of the experimentally derived structural parameters [12] agree with our DFT calculations within the experimental uncertainties, with only the average deviation of the y [001] coordinates of the CoO layer lying outside by 0.01 (O) and 0.02 Å(Co) [14]. Figure 1(a) presents the result of the fully relaxed calculations. In agreement with the experimental data, the oxide film is highly corrugated and displays a pronounced corrugation in terms of height differences of the O ($\sim$1 Å) and of the Co ($\sim$0.5 Å) atoms.

In this Letter, we also present a second stable overlayer geometry, constructed by shifting the overlayer by half the substrate Ir-Ir spacing in the [010] x direction [Fig. 1(b)]. In this structure, which is of different symmetry, the changes in the height of the O and Co atoms of the oxide film are less abrupt, although the corrugations are similar to the unshifted case. Surprisingly, the energy difference between the these two $c(10 \times 2)$ structures favoring the shifted structure [Fig. 1(b)] by 6 meV/Co atom is very small and negligible with respect to the expected accuracy. Note that a standard PBE calculation tilts the balance in favor of the unshifted structure [Fig. 1(a)] by 8 meV/Co atom. Therefore, the DFT calculations predict that both phases coexist under suitable experimental conditions. Experimentally, the two phases should be distinguishable by scanning tunneling microscopy because the simulated images are distinctly different: four bright spots (related to the uppermost oxygen atoms) are predicted for the originally proposed structure [12], whereas, for the new, registry-shifted structure five (or three) bright spots should appear. Indeed, very recent experimental measurements seem to confirm the coexistence of both structures [15].

The basic driving forces for the structural reconstruction can be analyzed in terms of a simplified, quasiepitaxial (SQE) model, where the hexagonal (111-like) CoO overlayer is accommodated on a square (100) substrate in a $p(1 \times 2)$ unit cell as shown in Fig. 2. In the energetically most favorable structure, the hexagonal CoO film binds to the substrate via both the Co1 and Co2 atoms and the on-top (O1) oxygen atoms at the corners of the supercell. Consequently, the Co1 and Co2 rows are pushed together by 0.53 Å compared to the ideal positions dictated by the substrate, thus, forming Co-O1-Co bond angles between 90° (Co1-O1-Co1) and 135° (Co1-O1-Co2), that resemble the quasihexagonal arrangement reminiscent of hex-BN networks. The second type of oxygen atoms (O2), located in bridge sites, is tilted out of the plane and hence, does not directly contribute to the bonding to the surface. The oxygen atoms display a O1-O2 buckling of 0.97 Å, forming a three sided pyramid with Co-O-Co bond angles close to 90° such as found in the bulk rock-salt structure along the [111] diagonal. Such a buckling is much less pronounced for the Co atoms, which are either located in hollow sites (Co1), with a vertical distance of 1.94 Å above the substrate, or in bridge sites (Co2), at a height of 2.27 Å [cf., Fig. 2(a)]. For comparison, a pure metallic Co overlayer on Ir(100) is also found to occupy hollow substrate sites at a height of 1.68 Å.

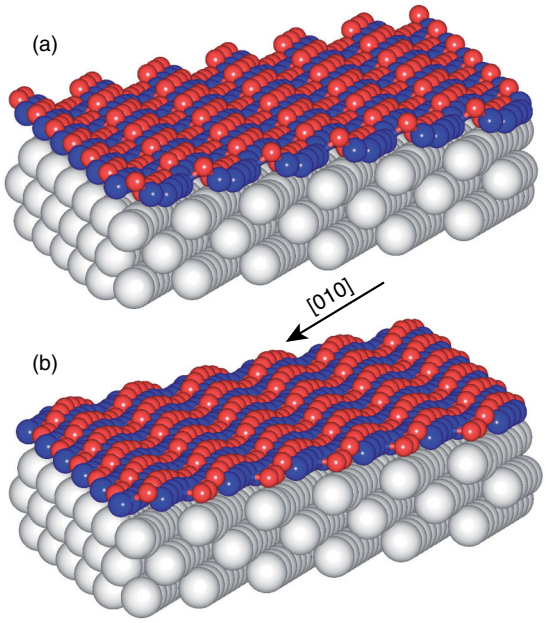

FIG. 1 (color online). Illustration of the calculated structure for a $c(10 \times 2)$ CoO(111) monolayer on Ir(100): O (red/gray), Co (blue/dark gray), Ir (white). (a) Experimentally proposed structure, (b) competing structure generated by shifting the CoO layer by half the Ir-Ir distance along the [010] direction. All directions [z, x, y] are given with respect to a (1×1) iridium cell. See also the positional data shown in Fig. 3.

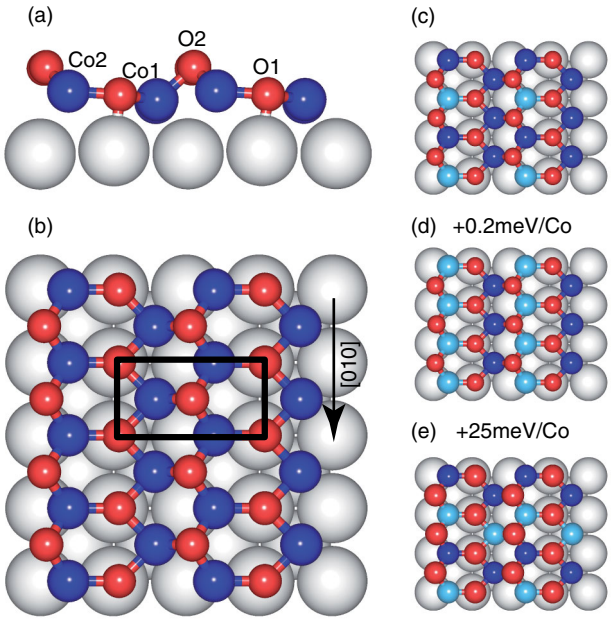

FIG. 2 (color online). SQE model of a hexagonal (1×1) CoO(111) monolayer on Ir(100): O (red/gray), Co (blue/dark gray), Ir (white). (a) Side view along [010] and (b) top view. (c)–(e) Different magnetic configurations, Co majority (blue/dark gray), Co minority (light blue/light gray). Configurations (c) and (d) are energetically almost degenerate (see text), while (e) is disfavored by 25 meV/Co atom.

The different coordination of the Co atoms is directly reflected in the magnetic ordering: the spin moments of the Co1 atoms in the hollow sites align ferromagnetically, comparable to the ferromagnetic order of the pure metallic Co overlayer [Fig. 2(c), dark blue (dark gray) atoms]. On the other hand, the magnetic order of the weaker bonded Co2 rows on the substrate bridge sites is less well defined: the difference in energy between the antiferromagnetic ordering and the ferromagnetic ordering *within* the Co2 rows—accompanied by an antiferromagnetic coupling to the Co1 rows—is only 0.2 meV per Co atom [Figs. 2(c) and 2(d)].

All other reasonable (collinear) magnetic orderings are unfavorable by at least 25 meV per Co atom, including antiferromagnetic alignments within the Co1 rows or ferromagnetic coupling of all Co atoms. The induced polarization on the nearby Ir atoms is small since the neighboring Co atoms have partially opposite magnetic moments. The same holds for the magnetism induced in the oxygen atoms. Therefore, we conclude that the Co atoms located on hollow sites have a strong tendency for *ferromagnetic* ordering along the chains, and *antiferromagnetic* coupling across the lines of O atoms to the bridge site Co2 chain. Applying the Kanamori–Goodenough–Anderson [16–18] rules in a simple way, one would predict a ferromagnetic coupling of the Co1 and Co2 chains connected by O2 atoms via direct Co1-Co2 overlap (Co1-O2-Co2 bond angles close to 90° and Co1-Co2 distance of 2.62 Å), while the coupling involving the planar O1 type atoms is less clear: the 90° Co2-O2-Co2 angles and a Co2-Co2 distance of 2.74 Å would again favor direct overlap ferromagnetic ordering along the Co2 rows, but the 135° Co1-O1-Co2 angles and Co1-Co2 distances of 3.56 Å would certainly work against ferromagnetic coupling, although antiferromagnetic coupling involving the O1 atom would be strongest for 180° angles. However, such a simple picture for the CoO film is certainly complicated by the interaction with the substrate, either by direct coupling of the Co spins via the substrate, or by changes in the oxygen orbitals caused by bonding to the substrate that would modify the superexchange interaction. Thus, the magnetic ordering observed for the CoO films should be characterized as a competition between ferromagnetic coupling between the Co atoms by direct overlap (and also mediated by the substrate) and antiferromagnetic coupling across oxygen atoms in the hex-BN like structures of the layer.

However, the small energy differences are of the same order as contributions from noncollinear spin arrangements. Since the full $c(10 \times 2)$ structure is too complex for a noncollinear study, we assess this possibility by performing calculations for selected noncollinear orderings between Co1 and Co2 spins based on the SQE model (Fig. 2). Considering Fig. 2(c) as a first step (corresponding to the collinear spin-polarized calculation), the collinear spin directions are fixed along [100] (out-of-plane) and then in a second step the FM Co1 or the AF Co2 spins are rotated by 90° perpendicular to [010] (in-plane). The energy gain for these noncollinear configurations is about 8 meV/Co. Estimating the coupling to the substrate, one finds that exchanging the spin axis of Co1 and Co2 favors a Co1 in-plane configuration, but only marginally by 0.6 meV/Co. Rotating the Co2 spins in-plane, while keeping the FM order [Fig. 2(d)], destabilizes the configuration by 20 meV/Co with respect to the one of Fig. 2(c). Therefore, it seems likely that noncollinear spin ordering occurs in the full $c(10 \times 2)$ structure, but that the magnetic coupling to the substrate plays only a minor role here.

The main patterns seen in the SQE model also hold for both of the much more complex cases of $c(10 \times 2)$ CoO overlayer structures on Ir(100) (see Fig. 4). Although the mismatch between the CoO film and the Ir(100) substrate leads to variations in the local configuration, the segments of the Co rows, either positioned on bridge-like or on hollow-like sites, are clearly visible in the fully relaxed structure (Fig. 3). However, as the $c(10 \times 2)$ CoO film is strained in the [010] x direction compared to the SQE model, there is a continuous transition from the hollow-like to the bridge-like Co segments, and hence, the Co atoms are not located in the ideal positions of the SQE model. Consequently, the chains in the [010] x directions get broken, when Co1 atoms are shifted from their ideal hollow positions to bridge positions; similar arguments holds for the Co2 chains. Therefore, the full model does not display infinite chains of one type of Co atoms along the [010] x direction, but rather alternating segments of both types arrange in a zigzag pattern (compare Figs. 3 and 4). Still, the height and in-plane modulations for both the O and Co atoms shown in Figs. 3(a)–3(c) match quite nicely the coordinates of the corresponding atoms of the SQE model which already captures the deviations from the ideal positions perpendicular to the Co/O chains ([001] y direction). Also, the agreement with the experimental LEED results [12,14] is excellent.

The predicted correlation between the spin alignment and the local geometry is also observed for the full model. For both CoO overlayer structures, the calculations show a particularly pronounced binding to the Ir substrate if the oxygen atoms are in on-top sites and the neighboring Co atoms are in hollow sites, forming anchor sites around which the less binding Co2 chain fractions are placed. This leads to the formation of two types of Co segments, a lower segment consisting of 4 (Co1) atoms in hollow positions, and a higher segment of 5 (Co2) atoms. As already observed in the SQE model, all Co1-like atoms are ferromagnetically aligned (Fig. 4, upper panel). Compared with the SQE model, we also predict antiparallel ordering of Co2 (bridge-like) atoms with an enhanced energy difference between anti- and parallel ordering

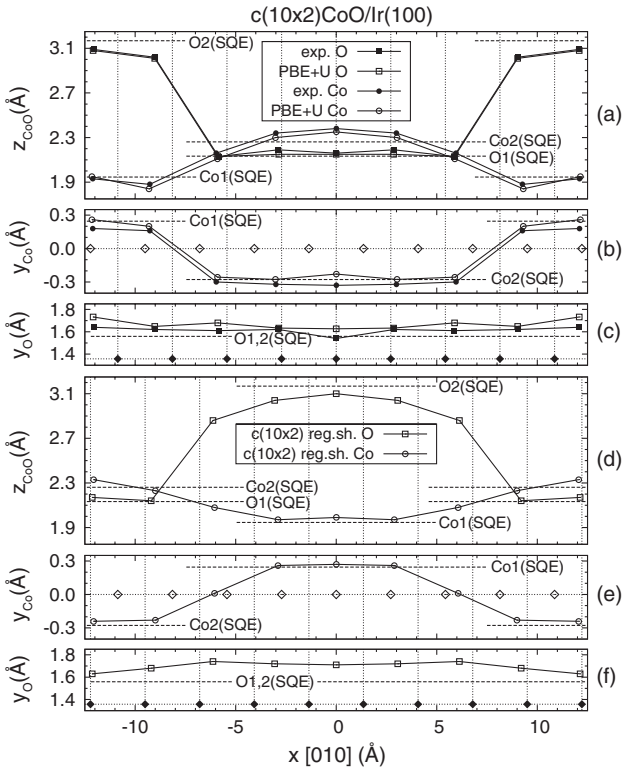

FIG. 3. Structural details of a hexagonal (1×1) CoO(111) monolayer on Ir(100). (a)–(c) Comparison between experiment and PBE + U (U-J = 1 eV) results. (d)–(f) CoO layer shifted by half of the substrate Ir-Ir spacing along x [010]. Thin vertical lines show the ideal lateral positions of the substrate Ir atoms along x [010], and empty (filled) diamonds show the ideal hollow (top) sites of the Ir substrate. For comparison, the "SQE" labeled dashed horizontal lines denote the atomic positions for the SQE model of Fig. 2. The z [100] (height) values for CoO in (a) and (d) are given with respect to the mean Ir positions in the interface layer, while in (b)–(c) and (e)–(f) the y [001] values are given with respect to the ideal hollow sites of the Ir substrate where Co atoms of a metallic Co overlayer would be found. To allow for a better comparison with experiments, the calculated lateral distances have been scaled to the experimental Ir lattice constant of 3.84 Å (theory: 3.88 Å).

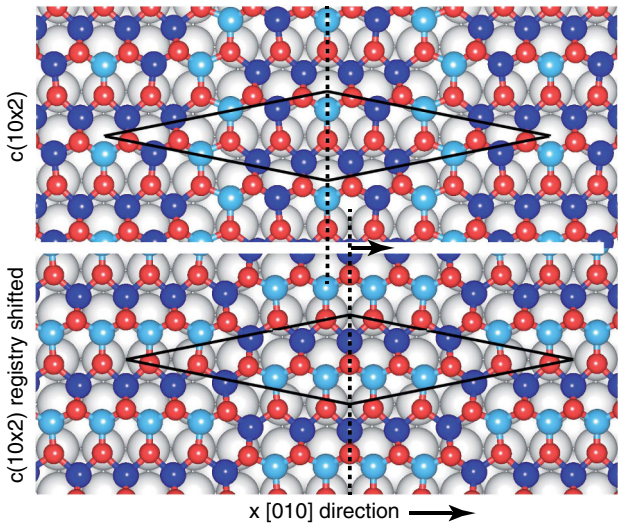

FIG. 4 (color online). Magnetic structure of a $c(10 \times 2)$ CoO(111) monolayer on Ir(100): O (red/gray), Co majority (blue/dark gray), Co minority (light blue/light gray), Ir (white). The top panel shows the experimentally proposed $c(10 \times 2)$ structure [12,14], the bottom panel shows a competing structure with a registry-shifted $c(10 \times 2)$ CoO overlayer, which is slightly favored by a 6 meV/Co atom.

within the *same* Co2 segment of 6 meV per Co atom. Therefore, it is likely that the atoms connecting the two different chain segments (Co1-like and Co2-like) have a noncollinear alignment. A very similar relation can be observed for the second, registry-shifted CoO structure (Fig. 4, lower panel). Due to the shift in the substrate lattice, there are now segments with an odd number of Co1 atoms (now 5) and an even number of Co2 atoms (now 4), and vice versa for the O atoms. For this geometry, the spin alignments are just the ones expected from the SQE model; i.e., all orderings *within* the chain segments are now parallel. As the noncollinear calculations for the SQE model show, a rotation of a *ferromagnetic* Co2 spin segment is unfavorable. Hence, noncollinear effects are expected to play a lesser role for the registry-shifted phase. Concerning the chain segments of the 5 high lying O atoms, the border atoms of these chains are lower in height because they are significantly shifted laterally towards the on-top substrate sites. Overall, this leads to a surface of smoother corrugation [cf., Figs. 1(b) and 3(d)–3(f)] compared to the unshifted case. Yet, the small energy difference between the plain registry-shifted $c(10 \times 2)$ phases can lead to the coexistence of both structures, and hence, incommensurate spin ordering.

In summary, we have investigated and analyzed the complex magnetic ordering in the supported $c(10 \times 2)$ CoO films on Ir(100). The calculations predict two closely related CoO overlayer phases, built up by Co segments consisting of either 4 or 5 atoms. We find a close relationship between the structural relaxations and the local magnetic ordering in the overlayer: the segments of Co atoms above hollow-like positions of Ir(100) clearly favor ferromagnetic coupling along the lines and antiferromagnetic coupling between the ferromagnetic rows, while the magnetic order is less pronounced in the segments with bridge-like atoms. Based on model calculations, noncollinear arrangements are expected to occur predominantly for the AF ordered chain segments. On the basis of these findings and their analysis, we expect a similar relationship between structure and magnetic ordering for related transition-metal oxide overlayers. Consequently, inducing a specific deformation by the coverage by the oxide overlayer may provide a strategy for designing magnetic properties of complex surface oxides.

Financial support by the Austrian Science Fund (FWF), SFB FOXSI (F45) and SFB VICOM (F41), as well as

by the National Science Foundation (DMR-0706359 and DMR-1105839) is gratefully acknowledged. We also appreciate the computer support of the Vienna Scientific Cluster (VSC).

*weinert@uwm.edu

[1] F. Allegretti, G. Parteder, L. Gragnaniello, S. Surnev, F. P. Netzer, A. Barolo, S. Agnoli, G. Granozzi, C. Franchini, and R. Podloucky, Surf. Sci. **604**, 529 (2010).
[2] C. Franchini, R. Podloucky, F. Allegretti, F. Li, G. Parteder, S. Surnev, and F. P. Netzer, Phys. Rev. B **79**, 035420 (2009).
[3] C. Franchini, J. Zabloudil, R. Podloucky, F. Allegretti, F. Li, S. Surnev, and F. P. Netzer, J. Chem. Phys. **130**, 124707 (2009).
[4] J. Klikovits *et al.*, Phys. Rev. Lett. **101**, 266104 (2008).
[5] N. Seriani and F. Mittendorfer, J. Phys. Condens. Matter **20**, 184023 (2008).
[6] F. Mittendorfer, J. Phys. Condens. Matter **22**, 393001 (2010).
[7] G. Kresse and J. Hafner, Phys. Rev. B **47**, 558 (1993).
[8] G. Kresse and J. Furthmüller, Comput. Mater. Sci. **6**, 15 (1996).
[9] G. Kresse and D. Joubert, Phys. Rev. B **59**, 1758 (1999).
[10] J. P. Perdew, K. Burke, and M. Ernzerhof, Phys. Rev. Lett. **77**, 3865 (1996).
[11] S. L. Dudarev, G. A. Botton, S. Y. Savrasov, C. J. Humphreys, and A. P. Sutton, Phys. Rev. B **57**, 1505 (1998).
[12] C. Ebensperger, M. Gubo, W. Meyer, L. Hammer, and K. Heinz, Phys. Rev. B **81**, 235405 (2010).
[13] C. Rödl, F. Fuchs, J. Furthmüller, and F. Bechstedt, Phys. Rev. B **79**, 235114 (2009).
[14] C. Ebensperger, Master's thesis, University of Erlangen, 2009 (in German).
[15] C. Tröppner, Ph.D. thesis, University of Erlangen, 2011 (in German); C. Tröppner *et al.* (to be published).
[16] J. Kanamori, J. Phys. Chem. Solids **10**, 87 (1959).
[17] J. B. Goodenough, Phys. Rev. **117**, 1442 (1960); J. B. Goodenough, *Magnetism and the Chemical Bond* (Interscience Publishers, New York, 1963).
[18] P. W. Anderson, Solid State Phys. **14**, 99 (1963).